SLAC-PUB-14522

Electric Field Penetration in Au/Nb:$SrTiO_3$ Schottky Junctions Probed by Bias-Dependent Internal Photoemission

Y. Hikita[1,a)], M. Kawamura[1], C. Bell[1], and H. Y. Hwang[1-3]

[1]*Department of Advanced Materials Science, University of Tokyo, Kashiwa, Chiba 277-8561, Japan*

[2]*Japan Science and Technology Agency, Kawaguchi, Saitama 332-0012, Japan*

[3] *Department of Applied Physics and Stanford Institute for Materials and Energy Science, Stanford University, Stanford, CA 94305, USA*

(Received)

Abstract

Electric field penetration into the metallic side of a Schottky junction is in principle a universal phenomenon, the magnitude of which increases with the semiconductor permittivity. Here, we quantitatively probe this effect using bias-dependent internal photoemission spectroscopy at the Schottky junction between a large dielectric permittivity semiconductor $SrTiO_3$ and gold. A clear linear reduction of the barrier height with increasing interface electric field was observed, highlighting the importance of field penetration into the gold. The interfacial permittivity of $SrTiO_3$ at the interface is reduced from the bulk value, reflecting intrinsic suppression at the interface.

[a)]Electronic mail: hikita@k.u-tokyo.ac.jp

Metal-semiconductor Schottky junctions are ideal platforms for studying the fundamental physics of carrier transport across heterojunctions, as well as being one of the most basic building blocks for practical electronic devices. With the current movement towards advanced functionality in complex oxide devices, various studies have examined the high sensitivity of perovskite Schottky junctions to external perturbations such as magnetic field[1,2], light irradiation[3] and electric field[4]. Furthermore, by applying atomic scale growth techniques in oxide thin films, oxide Schottky barrier heights (SBH) can be modulated by tuning interface dipoles[5] and introducing resonant artificial interface states[6]. Despite such progress, there is still a basic need to develop a quantitative description of the interface band structure, which determines the device operation in these systems.

Junctions utilizing $SrTiO_3$ as the semiconductor have been the most commonly fabricated perovskite structure, due to the accessibility of high quality single crystals with well-controlled doping. $SrTiO_3$ is an incipient ferroelectric, characterized by its strong electric field and temperature dependent dielectric permittivity[7,8] $\varepsilon_S(E,T)$. In $SrTiO_3$ Schottky junctions, $\varepsilon_S(E, T)$ modifies band bending from the familiar quadratic form to an exponential form, leading to quadratic corrections to the linear $1/C^2$ - V relationship typical in semiconductors with constant permittivity[9,10]. Here C is the depletion capacitance and V the applied voltage across the Schottky junction.

Another important feature of an incipient ferroelectric is the magnitude of the dielectric permittivity ε_S, ~$276\,\varepsilon_0$ in $SrTiO_3$ at room temperature[9], far larger than conventional semiconductors ($11\,\varepsilon_0$ in Si; ε_0 is the vacuum permittivity). This large permittivity, in principle, causes a voltage drop on the metal side [Fig. 1(a)] due to the

conservation of the electric displacement (Gauss' law). This effect was theoretically proposed more than forty years ago[11] based on the early studies of metal/dielectric interfaces[12-16], and it was suggested that it should be dominant over image force or tunneling contributions in the limit of large ε_S. Practically, however, this effect is negligible in conventional semiconductors, and the assumption of perfect screening in the abrupt junction approximation provides a quantitatively accurate band diagram. In this study, we used internal photoemission (IPE) under applied DC bias to measure the electric field penetration at a Au/Nb-doped $SrTiO_3$ (Nb:$SrTiO_3$) Schottky junction. IPE is one of the few techniques capable of directly spectroscopically probing the SBH under applied DC bias. These measurements reveal a significant reduction in the SBH ($-\Delta\Phi_{SB}$) under reverse bias, indicating a dominant contribution from electric field penetration, rather than image force effects due to electron transport across the interface[17] [Fig.1(b)].

The most challenging technical requirement to measure the bias-dependence of the SBH is to maximize the voltage range over which data can be taken. A large reverse bias leakage current can hinder the measurement by 1) not applying the full voltage to the junction, and 2) by reducing the signal-to-noise ratio in the usual phase-sensitive detection scheme. It is known that the current-voltage (*I*-*V*) characteristics of Au/Nb:$SrTiO_3$ junctions are degraded by carbon contaminants on the Nb:$SrTiO_3$ surface, and that these can be removed by annealing in highly oxidizing conditions such as ozone atmosphere[18], or by pre-evaporating bismuth metal on the surface followed by annealing in oxygen ambient[19,20]. In the latter method, the carbon contaminants simultaneously evaporate with bismuth when the substrate is heated. Here, we applied this second procedure, followed by annealing in an RF radical-activated oxygen ambient to further

improve the junction characteristics and to fully compensate for possible reduction at the surface of $Nb:SrTiO_3$.

We evaporated bismuth metal onto a 5 mm×5 mm×0.5 mm $Nb:SrTiO_3$ (001) single crystal substrate under a background pressure of 1.0×10^{-5} Pa. The substrate was then loaded into a vacuum chamber and annealed at 500 ^{o}C for 60 minutes, in an ambient of RF radical-activated oxygen gas at a pressure of 5×10^{-5} Torr. After evaporating the gold in situ, the electrode contacts were made with silver epoxy on the Au and an ultrasonic solder of In-Ga on the $Nb:SrTiO_3$ side. The voltage was applied with respect to the $Nb:SrTiO_3$ electrode. The lowest commercially available niobium concentration of 0.01 wt. % was used to minimize the reverse bias tunneling current.

Figure 2(a) shows the *I-V* characteristics for the surface treated and non-treated junctions. A dramatic reduction in the reverse bias current is evident by the bismuth surface cleaning. By applying the thermionic emission model to the forward bias region, we observed an improvement in the ideality factor from 1.6 to 1.2. Assuming a Richardson constant of 156 A/cm^2 (Ref. [21]), the SBH obtained for the treated sample is 1.46 V. The *C-V* characteristics, also shown in Fig. 2(a), shows a linear relation between $1/C^2$ and the applied voltage, giving a built-in potential V_{bi} of 1.42 V and a dopant concentration N_{D} of 8.0×10^{17} cm^{-3} using

$$\frac{1}{C^2}=\frac{2}{\varepsilon_0\varepsilon_{\mathrm{S}}qN_{\mathrm{D}}}\left(V_{\mathrm{bi}}-V\right). \tag{1}$$

Here q is the elementary charge. The obtained dopant concentration is in close agreement with the carrier density of 1×10^{18} cm^{-3} from Hall measurements[21] confirming negligible surface reduction during bismuth surface treatment. The 25 % reduction in N_{D} from the

nominal value 3.3×10^{18} cm^{-3} is commonly reported for 0.01 wt. % Nb:$SrTiO_3$, and is caused by the partial deactivation of the donors[22]. Using these experimentally obtained values, the equilibrium electric field at the interface E_m is calculated to be 3.9×10^{5} V/cm following $E_\mathrm{m}=\sqrt{2qN_\mathrm{D}\left(V_\mathrm{bi}-V\right)/\varepsilon_\mathrm{S}\varepsilon_0}$.

The result of IPE measurements under bias is shown in Fig. 2(b); the experimental details are given in Ref. 21. As can be seen, the data in the vicinity of the SBH are very well described by the Fowler relation, $\sqrt{Y}\sim h\nu-\Phi_\mathrm{m}(V)$, where Y is photoyield, $h\nu$ the incident photon energy, and $\Phi_\mathrm{m}(V)=\Phi_\mathrm{SB}-\Delta\Phi_\mathrm{SB}(V)$ is the measured SBH under bias. Φ_m at zero bias is 1.47 V, in excellent agreement with V_bi obtained from the C-V characteristics and I-V data. The bias-dependence of the SBH is relatively large, decreasing by 0.04 V at an applied bias of -3.2 V. The SBH reduction under bias is typically associated with the image force effect expressed as $-\Delta\Phi_\mathrm{SB}=\sqrt{E_\mathrm{m}/4\pi\varepsilon_0\varepsilon_\mathrm{if}}$, from which the interfacial permittivity ε_if can be obtained. As shown in the inset of Fig. 3, a direct fit of the data with respect to $\sqrt{E_\mathrm{m}}$ gives $\varepsilon_\mathrm{if}=1.1$, which is unphysically low compared to the bulk DC permittivity or even the optical dielectric permittivity ~5.8 of $SrTiO_3$ (Ref. 23). Thus image force barrier reduction clearly cannot be the dominating cause of the observed bias-dependent SBH.

In Fig. 3, $-\Delta\Phi_\mathrm{SB}$ is plotted against E_m. Continuity of the electric displacement requires that $-\Delta\Phi_\mathrm{SB}/\lambda_\mathrm{TF}=\varepsilon_\mathrm{if}E_\mathrm{m}$. Here we assume a Thomas-Fermi screening length in gold of λ_TF = 0.06 nm, estimated from the free electron approximation[13]. By incorporating an experimentally determined estimate for the dielectric permittivity of gold ε_M = 6.9 (Ref. 24), a fit to the experimental data gives ε_if = 195 ± 15, which is

similar to the bulk permittivity, indicating the dominance of the field penetration effect at this junction. In detail, the ~ 30 % reduction from the bulk permittivity can be attributed to the small electric field dependence in the permittivity expected for a lightly doped (< 10^{19} cm^{-3}) Nb:$SrTiO_3$. The range in $\varepsilon_{\mathrm{if}}$ takes into account a conservative estimate of 10 % variation in ε_{M} or λ_{TF}. These results give direct experimental evidence for the suppressed permittivity at the interface, which has been discussed to be the origin for the non-ideal *I-V* characteristics in Nb:$SrTiO_3$ Schottky junctions[18] and the dielectric dead layer at metal/$SrTiO_3$ thin film interfaces studied from first-principles calculations[25].

Given the large permittivity found in many oxide semiconductors, the concept of field penetration is widely applicable to many oxide-based heterostructures, including functional devices[26] and nanoscale metal-oxide catalysis systems[27]. In such studies, IPE should be effective not only to provide a direct measure of the band offsets, but also to enable access to critical physical properties buried at the interface.

YH acknowledges support from the Futaba Foundation and the Asahi Glass Foundation. HYH acknowledges the Department of Energy, Office of Basic Energy Sciences, Division of Materials Sciences and Engineering, under contract DE‐AC02‐76SF00515.

References

1. N. Nakagawa, M. Asai, Y. Mukunoki, T. Susaki, and H. Y. Hwang, Appl. Phys. Lett. **86**, 082504 (2005).
2. J. Matsuno, A. Sawa, M. Kawasaki, and Y. Tokura, Appl. Phys. Lett. **92**, 122104 (2008).
3. Y. Muraoka and Z. Hiroi, J. Phys. Soc. Jpn **72**, 781 (2003).
4. A. Sawa, Mater. Today **11**, 28 (2008).
5. Y. Hikita, M. Nishikawa, T. Yajima, and H. Y. Hwang, Phys. Rev. B **79**, 073101 (2009).
6. Y. Hikita, L. Fitting Kourkoutis, T. Susaki, D. A. Muller, H. Takagi, and H. Y. Hwang, Phys. Rev. B **77**, 205330 (2008).
7. E. Sawaguchi, A. Kikuchi, and Y. Kodera, J. Phys. Soc. Jpn. **17**, 1666 (1962).
8. M. A. Saifi and L. E. Cross, Phys. Rev. B **2**, 677 (1970).
9. T. Yamamoto, S. Suzuki, K. Kawaguchi, and K. Takahashi, Jpn. J. Appl. Phys. **37**, 4737 (1998).
10. T. Susaki, Y. Kozuka, Y. Tateyama, and H. Y. Hwang, Phys. Rev. B **76**, 155110 (2007).
11. S. S. Perlman, IEEE Trans. Electron Devices **ED-16**, 450 (1969).
12. C. A. Mead, Phys. Rev. Lett. **6**, 545 (1961).
13. H. Y. Ku and F. G. Ullman, J. Appl. Phys. **35,** 265 (1964).
14. A. Braunstein, M. Braunstein, G. S. Picus, and C. A. Mead, Phys. Rev. Lett. **14**, 219 (1965).
15. G. W. Lewicki and C. A. Mead, Appl. Phys. Lett. **8**, 98 (1966).

16. C. A. Mead, Appl. Phys. Lett. **9**, 53 (1966).
17. S. M. Sze, C. R. Crowell, and D. Kahng, J. Appl. Phys. **35**, 2534 (1964).
18. T. Shimizu and H. Okushi, J. Appl. Phys. **85**, 7244 (1999).
19. S. Watanabe, T. Hikita, and M. Kawai, J. Vac. Sci. Technol. A **9**, 2394 (1991).
20. T. Hikita, T. Hanada, M. Kudo, and M. Kawai, J. Vac. Sci. Technol. A **11**, 2649 (1993).
21. Y. Hikita, Y. Kozuka, T. Susaki, H. Takagi, and H. Y. Hwang, Appl. Phys. Lett. **90**, 143507 (2007).
22. T. Fujii, M. Kawasaki, A. Sawa, Y. Kawazoe, H. Akoh, and Y. Tokura, Phys. Rev. B **75**, 165101 (2007).
23. W. L. Bond, J. Appl. Phys. **36**, 1674 (1965).
24. I. N. Shklyarevskii and P. L. Pakhomov, Opt. Spectrosc. **34**, 90 (1973).
25. M. Stengel and N. A. Spaldin, Nature **443**, 679 (2006).
26. T. Yajima, Y. Hikita, and H. Y. Hwang, Nature Mater. **10**, 198 (2011).
27. K. Mitsuhara, Y. Kitsudo, H. Matsumoto, A. Visikovskiy, M. Takizawa, T. Nishimura, T. Akita, and Y. Kido, Surf. Sci. **604**, 548 (2010).

Figure Captions:

Fig. 1: (Color online) Schematic band diagram of a Au/Nb:$SrTiO_3$ junction under reverse bias showing (a) electric field penetration and (b) image force barrier lowering. E_F is the gold Fermi level, E_C the $SrTiO_3$ conduction band minimum, V_{bi} the built-in potential, and $\Delta\Phi_{SB}$ is the SBH variation from the intrinsic SBH Φ_{SB}.

Fig. 2: (Color online) (a) *I-V* characteristics of the Au/Nb:$SrTiO_3$ Schottky junction with (red squares) and without (blue circles) bismuth surface treatment. *C-V* characteristics of the bismuth surface treated junction (red triangles). The solid line indicates a linear fit using Eq. (1). (b) Square-root of the photoyield against the incident photon energy near the SBH taken under various applied bias voltages. Solid lines indicate linear extrapolations.

Fig. 3: (Color online) Schottky barrier height reduction ($-\Delta\Phi_{SB}$) as a function of the electric field at the interface E_m. The solid line denotes the linear fit to the experimental data. The dotted (blue) line shows the calculated SBH lowering due to field penetration based on the bulk dielectric permittivity. The inset shows $-\Delta\Phi_{SB}$ as a function of $\sqrt{E_m}$ with a fit (solid line) assuming image force barrier reduction.

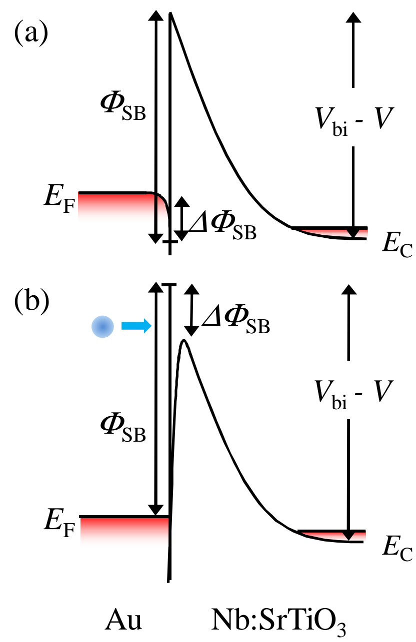

Fig. 1 Y. Hikita *et al.*

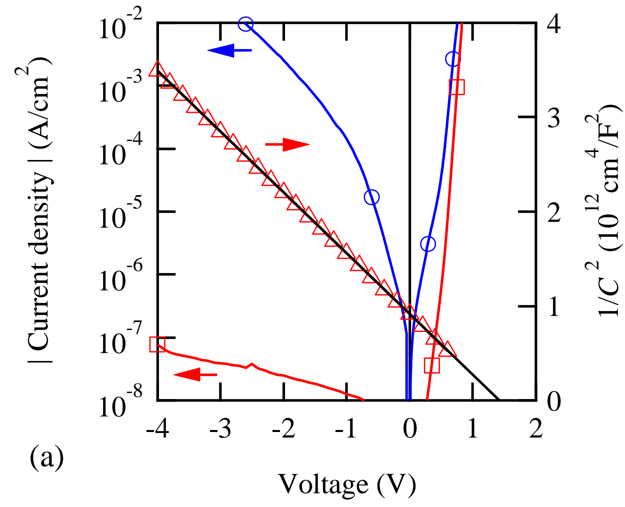

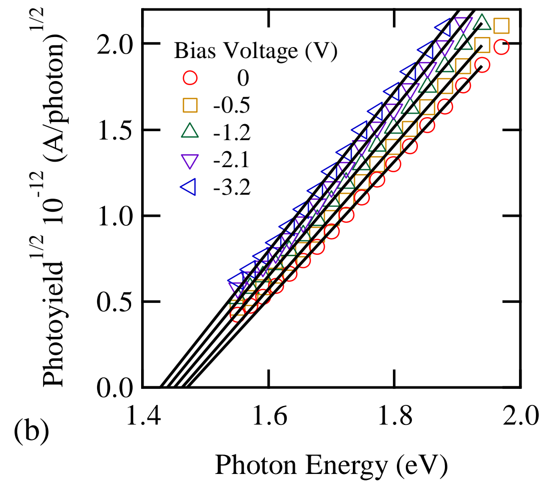

Fig. 2 Y. Hikita *et al.*

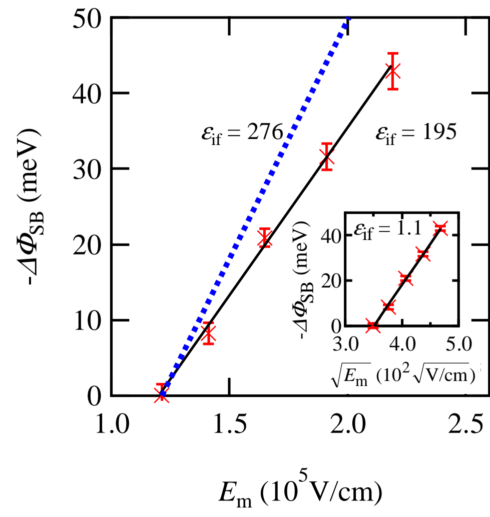

Fig. 3 Y. Hikita *et al.*